Struct Chem
DOI 10.1007/s11224-016-0863-1

ORIGINAL RESEARCH

Experimental and theoretical investigation of new furan and thiophene derivatives containing oxazole, isoxazole, or isothiazole subunits

Pervin Ünal Civcir[1] · **Gülbin Kurtay**[1] · **Kübra Sarıkavak**[1]

Received: 4 April 2016 / Accepted: 12 October 2016

Abstract Herein, we present joint experimental and theoretical studies on newly designed thiophene- or furan-based oxazole, isoxazole, and isothiazole derivatives. Our synthetic approach towards the preparation of target compounds is based on Van Leusen reaction. By following this reaction, oxazoles (**1** and **2**) containing the pertinent heterocyclic systems were obtained from the reaction of suitable furan or thiophene derivatives with tosylmethyl isocyanide (TOSMIC). Hereby, three ring systems of furan or thiophene, linked to the oxazole rings at their 2- and 5-positions (**3** and **4**), were also successfully synthesized for the first time. Reaction of the starting materials containing acetyl groups in their 2-position with dimethyl acetal and following the treatment by hydroxylamine hydrochloride, desired isoxazole derivatives (**5** and **6**), were obtained. Additionally, isothiazole derivatives (**7** and **8**) were prepared by following the similar approach to the isoxazole synthesis. Whole of these cyclization reactions occurred with good to excellent yields. Structural analyses of the synthesized compounds were performed by appropriate spectroscopic methods (UV-vis, FT-IR, LC-MS, ^{1}H-NMR, ^{13}C-NMR, and elemental analysis). We also carried out theoretical studies for identifying the structure-activity relationship and determining chemical properties of the studied molecules. For this purpose, we obtained information about structural properties (bond lengths, bond angles, dihedral angles, and dipole moments), band gap energies, and spectroscopic characteristics (UV-vis, FT-IR, ^{1}H-NMR, and ^{13}C-NMR) of the target compounds.

Keywords Oxazole · Isoxazole · Isothiazole · Thiophene · Furan · DFT

Introduction

Heterocyclic azole compounds exhibit important role in broad variety of physiological cell processes by the contribution of their good solubility in water and relatively high thermal stability with respect to other heteroaromatic systems. In addition, azoles are acceptable as synthons in the preparation of natural products, pharmaceuticals, and dyes [1–3]. These compounds are also used in industrial applications such as corrosion inhibitor or catalyst for polymerization processes [4–7]. Moreover, researchers have been using oxazole derivatives especially as an antibiotic and anti-proliferative agent [8–12]. Among the biological activities of the oxazole nucleus containing drug intermediates, anti-inflammatory [13, 14], analgesic [15, 16], antibacterial [17–19], antifungal [20–22], anti-tuberculosis [23, 24], muscle relaxant [25], and HIV inhibitory [26] properties could also be considered. Besides, isoxazoles are widely used in various heterocyclic compounds synthesis and their antibacterial [27–29], antimicrobial [30–32], anticonvulsant [33–35], anthelmintic [36, 37], and cholesterol-lowering [38] properties are well-known. Similar to oxazole and isoxazole derivatives, isothiazole ring containing compounds show also biological activity [38, 39] and are used in the treatment of schizophrenia and for instance it could be found in the structure of ziprasidone [40] and perospirone [41]. Nowadays, azole derivatives are prepared by using different synthetic approaches [42]. In the scope of this research,

Electronic supplementary material The online version of this article (doi:10.1007/s11224-016-0863-1) contains supplementary material, which is available to authorized users.

✉ Pervin Ünal Civcir
pervin.unal.civcir@science.ankara.edu.tr; pcivcir@yahoo.com.tr

[1] Department of Chemistry, Faculty of Science, Ankara University, 06100 Ankara, Turkey

Published online: 14 November 2016

these above-mentioned facts induced us to synthesize some of newly oxazole, isoxazole, and isothiazole derivatives (Fig. 1) possessing a thiophene (or furan) ring systems which contain a methyl group at their 5-position in order to prevent further polymerization reactions [43]. As mentioned before, the target compounds were composed of different ring systems. Consequently, their synthesis methods also varied. According to the Van Leusen reaction [44], oxazoles containing furan or thiophene were obtained in very good yields from the reaction of suitable starting materials—furan or thiophene containing an aldehyde group at their 2-position with TOSMIC [45]. Similarly, the furan or thiophene derivatives containing two oxazole rings at their 2- and 5-positions were also synthesized successfully. Reaction of the starting materials containing acetyl groups in their 2-position with dimethylacetal, in the presence of N,N-dimethylformamide and following the treatment by hydroxylamine hydrochloride, isoxazole derivatives were obtained in good yields. Isothiazole derivatives were prepared by a similar to isoxazole synthesis method but consisted of four steps. These molecule series were also obtained in high yields. Structural analysis of the synthesized compounds was performed with appropriate spectroscopic methods.

In this study, we also aimed at identifying structural-activity relationship, determining some properties and comparing the experimental and theoretical properties of the target compounds. Therefore, the structural, chemical, electronic, and spectral characteristics of target compounds were investigated with both experimental and theoretical methods. Synthesis and theoretical studies of target compounds were performed simultaneously.

Materials and methods

Materials

N,N-Dimethylformamide (DMF) was dried over 4A molecular sieves (8–12 mesh) and freshly distilled under vacuum just before use. Anhydrous potassium carbonate and drying agents (sodium sulfate and magnesium sulfate) were pre-dried and activated in a hot air oven at 150 °C for 2 to 4 h. Super-dry ethanol was prepared from commercially available absolute ethanol. For this purpose, absolute ethanol was refluxed for 1 h in the presence of magnesium and catalytic amount of iodine. After that, the mixture was warmed until the iodine color totally disappeared. The resulting mixture was distilled off directly into the receiving flask and was stored over activated 4A molecular sieves. All of the other solvents used in this study, dichloromethane (DCM), N,N-dimethylformamide dimethylacetal (DMFDMA), diethyl ether, chloroform, methanol, ethyl acetate, and hexane, were stored over a suitable drying agent (usually 4A molecular sieves) under oxygen-free nitrogen. Reagents and catalyzers used during the experiments, 5-methyl-2-thiophenecarboxaldehyde, 5-methyl-2-furancarboxaldehyde, thiophene-2,5-dicarboxaldehyde, furan-2,5-dicarboxaldehyde, TOSMIC, hydroxylamine hydrochloride, phosphoryl chloride, sodium sulfide nonahydrate, and hydroxylamine-o-sulfonic acid (HSA), were used as received from *Sigma-Aldrich* without any further purification unless otherwise specified.

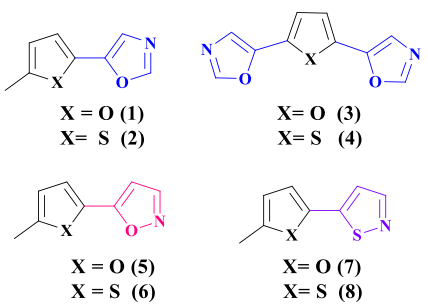

Fig. 1 Synthesized oxazole (**1**, **2**, **3**, **4**), isoxazole (**5**, **6**), and isothiazole (**7**, **8**) derivatives

Instrumentation

The FT-IR spectra were acquired on a Perkin-Elmer Spectrum 100 Series FT-IR spectrometer (Perkin Elmer Co., Beaconsfield, Bucks, and UK). Measurements were performed in KBr pellets or in ATR mode using the average of 15 scans. The UV–vis spectra were obtained on a Shimadzu UV-2550 double beam spectrophotometer (Shimadzu Corporation, Tokyo, Japan) utilizing quartz cuvettes of 1 cm path length between the wavelength range of 200 and 800 nm and all measurements were performed at room temperature. ^{1}H-NMR and ^{13}C-NMR spectra were recorded at room temperature on a Varian-Mercury 400 MHz high performance digital Fourier Transform (FT)-NMR Spectrometer (Mercury-400BB) (Varian, Fort Collins, CO, USA) and $CDCl_3$ was utilized as solvent. The ^{1}H-NMR chemical shifts were reported as δ values in parts per million (ppm) relative to tetramethylsilane (TMS, δ: 0) as internal standard. Proton coupling patterns were described as singlet (s), doublet (d), triplet (t), quartet (q), pentet (p), sextet (h), multiplet (m), and broad (br). Coupling constants J were given in Hz. The ^{13}C-NMR chemical shifts were also reported as δ values in ppm downfield from TMS. LC-MS spectra were taken by using a Waters-2695 Alliance HPLC system (Waters Corporation, Milford, MA, USA) equipped with DAD detector at 254 nm was coupled to a Micromass ZQ 2000 electrospray mass spectrometer. Elemental analyses were carried out with a Eurovector EA3000 CHNS elemental analyzer (EuroVector SpA, Italy) and found to be within a range of ±0.4 % of theoretical values. Thin layer chromatography (TLC) was used to observe the progress of the experiments. For this purpose, aluminum sheets (Merck, 20 × 20, Silica Gel 60 F254)

were selected. Purification of the products from common impurities—including byproducts, unreacted starting materials, etc.—was carried out by column chromatography or flash chromatography techniques. For this purpose, silica gel (SiO_2) (Merck, Silica Gel 60, 0.063–0.200 mm, 70–230 mesh ASTM) was used as the column stationary phase.

Synthetic procedures

In this study, we focused on the preparation of new isothiazole, oxazole, and isoxazole derivatives containing furan or thiophene units as heterocyclic system. As mentioned before, we designed our molecules with a blockage unit in their α-position of the corresponding heteroaromatic ring in order to prevent further polymerization reactions. Detailed experimental procedures were schematized and described below.

Synthesis of oxazole derivatives

In accordance with Van Leusen reaction, the target oxazole derivatives (1–4) including thiophene or furan ring systems were prepared by the following method. Method A consists of one-step ring closure reaction (Scheme 1).

Method A

Into a round bottomed flask fitted with a reflux condenser and dropping funnel, appropriate starting material (5-methyl-2-furancarboxaldehyde, 5-methyl-2-thiophenecarboxaldehyde, furan-2,5-dicarboxaldehyde, or thiophene-2,5-dicarboxaldehyde) (4.0 mmol) was introduced and the reaction was performed under nitrogen atmosphere and an ice bath was used in order to maintain the reaction temperature at around 5 °C. Previously dried K_2CO_3 (8.0 mmol) and methanol (5 mL) were added to the reaction flask with vigorous stirring. Then, TOSMIC (4.5 mmol) was dissolved in methanol (10 mL) and added slowly to the mixture via the dropping funnel over a period of 1 h. After completing additions, the

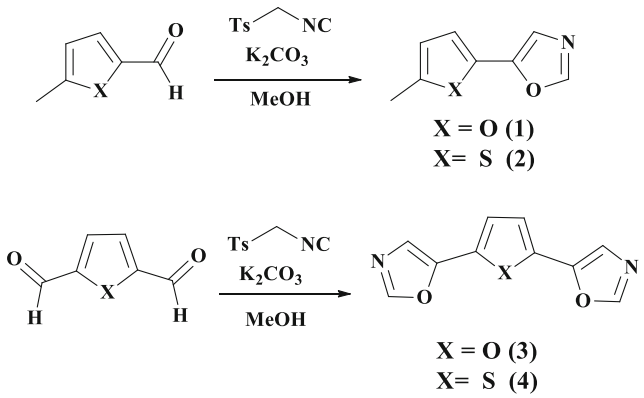

Scheme 1 Synthetic route to oxazole derivatives (**1–4**)

reaction mixture was allowed to stir for about 30 min, then the ice bath was removed and the system was heated in an oil bath to 70 °C. The reaction was followed by thin layer chromatography (TLC) and the experiment was terminated after ~6 h. The flask was cooled down to the room temperature and stirred for an extra 10 min following by the addition of 10 mL pure water. The resulting yellowish colored solution was extracted with dichloromethane (2 × 30 mL). The extracts were washed with water (3 × 10 mL) and saturated NaCl solution (3 × 10 mL), respectively. The combined organic phase was dried over $MgSO_4$. After filtration, dichloromethane was removed by a rotary evaporator to yield oily products.

5-(5-Methylfuran-2-yl)oxazole (1): (72 %), yellow colored oily product ^{13}C-NMR (400 MHz, $CDCl_3$) δC/ppm: 13.5, 107.6, 108.6, 120.4, 141.6, 144.2, 149.6, 153.2. ^{1}H-NMR (400 MHz, $CDCl_3$) δH/ppm: 2.3 (s, 3H, methyl –CH_3), 6.1 (m, 1H), 6.5 (d, J = 3.2 Hz, 1H), 7.1 (s, 1H), 7.8 (s, 1H). MS (EI) m/z (%) calcd. for $C_8H_7NO_2$: 149.15; found: 150.14 (M+, 100) (LC): 5.64 min. (100 % ionization peak). IR (ATR), ν_{max}/cm^{-1}: 3140 (w, aromatic C-H stretching), 1635 (w, C=C stretching), 1585 (w, C=N stretching), 1204, 1105, 1082 (m, C-O stretching), 785 (s, C-H bending).

5-(5-Methylthiophene-2-yl)oxazole (2): (yield: 69 %), bright yellow colored oily product ^{13}C-NMR (400 MHz, $CDCl_3$) δC/ppm: 15.2, 120.4, 124.6, 125.9, 127.1, 140.9, 147.1, 149.5. ^{1}H-NMR (400 MHz, $CDCl_3$) δH/ppm: 2.5 (s, 3H, methyl –CH_3), 6.7 (m, 1H), 6.5 (p, J = 4.8 Hz, 1H), 7.0 (t, J = 3.6 Hz, 2H), 7.8 (s, 1H). MS (EI) m/z (%) calcd. for C_8H_7NOS: 165.21; found: 207.14 (M + H + CH_3CN), 166.10 (M + H) (LC): 5.99 min. (100 % ionization peak). IR (ATR), ν_{max}/cm^{-1}: 3124, 3074 (w, aromatic C-H stretching), 2920, 2857 (w, aliphatic C-H stretching), 1611 (w, aromatic C=C stretching), 1503 (w, aromatic C=N stretching), 1259 (w, C-O stretching), 1090 (m, C-O-C stretching), 796 (s, C-H bending).

2,5-Bis(oxazol-5-yl)furan (3): (yield: 80 %) bright yellow colored oily product ^{13}C-NMR (400 MHz, $CDCl_3$) δC/ppm: 109.3, 122.3, 143.2, 143.6, 150.2. ^{1}H-NMR (400 MHz, $CDCl_3$) δH/ppm: 6.7 (s, 2H), 7.3 (s, 2H), 7.9 (s, 2H). MS (EI) m/z (%) calcd. for $C_{10}H_6N_2O_3$: 202.17; found: 244.45 (M + H + CH_3CN), 203.31 (M + H) (LC): 4.22 min. (100 % ionization peak). IR (ATR), ν_{max}/cm^{-1}: 3101, 2955, 2916, 2849 (m, aromatic C-H stretching), 2916, 2849 (m, aliphatic C-H stretching), 1516 (w, aromatic C=C stretching), 1456 (w, C=N stretching), 1203 (w, C-O stretching), 801 (s, C-H bending).

2,5-Bis(oxazol-5-yl)thiophene (4): (yield: 53 %) yellow-orange colored oily solid ^{13}C-NMR (400 MHz, $CDCl_3$) δC/ppm: 121.2, 125.1, 129.6, 146.2, 150.1. ^{1}H-NMR

(400 MHz, $CDCl_3$) δH/ppm: 7.2 (s, 2H) 7.3 (s, 2H), 7.8 (s, 2H). MS (EI) m/z (%) calcd. for $C_{10}H_6N_2O_2S$: 218.23; found: 260.06 (M + H + CH_3CN), 219.06 (M + H) (LC): 4.18 min. (100 % ionization peak). IR (ATR), ν_{max}/cm^{-1}: 3117 (w, aromatic C-H stretching), 1659, 1611 (w, aromatic C=C stretching), 1518, 1491 (w, C=N stretching), 1012 (m, C-O stretching), 802 (s, C-H bending).

Synthesis of isoxazole derivatives

The target isoxazole derivatives (5 and 6) were obtained by using Method B. First step of the process consisted of the reaction of the convenient starting materials with N,N-dimethylformamide dimethylacetal and the second step included the addition of hydroxylamine hydrochloride in the presence of methyl alcohol (Scheme 2).

Method B

First step Into a 100 mL of round bottom flask equipped with reflux condenser and dropping funnel; appropriate starting material (5-methyl-2-furancarboxaldehyde or 5-methyl-2-thiophenecarboxaldehyde) (5.5 mmol) was added and the reaction flask was placed into an ice bath. Following the addition of DMFDMA (5.5 mmol, d: 0.897 g/mL), the color of the solution turned yellow to orange and then burgundy. The ice bath was removed after 1 h of vigorous stirring and the mixture was heated in an oil bath to 110 °C. Eight hours later, with the aid of the one-dimensional TLC analysis, the experiment was terminated. After then, the system was cooled to room temperature and the flask was allowed to stand in a salt-ice bath. The crude products were crystallized from o-xylene.

(E)-3-(Dimethylamino)-1-(5-methylfuran-2-yl)prop-2-en-1-one (i): (yield: 81 %, m.p: 126–128 °C) dark brown crystals ^{1}H-NMR (400 MHz, $CDCl_3$) δH/ppm: 2.2 (s, 3H, methyl –CH_3), 2.8 (s, 3H), 3.1 (s, 3H), 5.6 (d, J = 12.4 Hz, 1H), 6.1 (q, J = 2.8 Hz, 1H), 6.9 (d, J = 3.6 Hz, 1H), 7.7 (d, J = 12.8 Hz, 1H). IR (ATR), ν_{max}/cm^{-1}: 3105 (w, aromatic C-H stretching), 2916, 2287 (w, aliphatic C-H stretching), 1737 (w, C=O stretching), 1633, 1546 (aromatic C=C stretching), 1263 (s, C-N stretching), 1068 (s, C-O stretching), 947 (m, =C-H twisting), 779 (s, aromatic C-H bending). Elemental analysis: anal. calcd. for $C_{10}H_{13}NO_2$ (179.2): C 67.02 H 7.31 N 7.82; found: C 66.81 H 7.17 N 7.43.

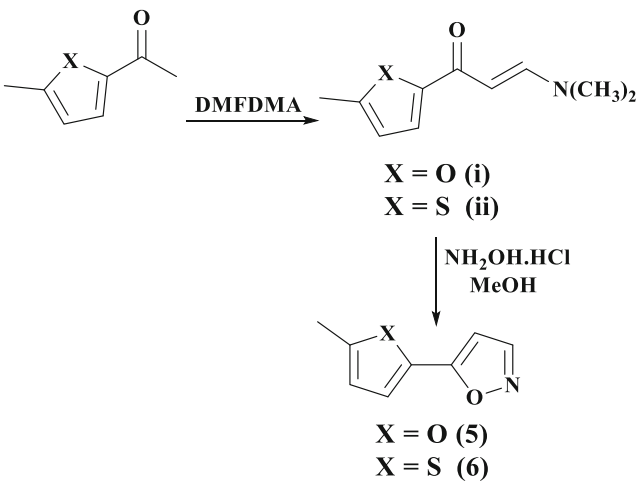

Scheme 2 Synthetic route to isoxazole derivatives (**5**–**6**)

(E)-3-(Dimethylamino)-1-(5-methylthiophene-2-yl)prop-2-en-1-one (ii): (39 %, m.p: 135 °C) brown crystals ^{1}H-NMR (400 MHz, $CDCl_3$) δH/ppm: 2.4 (d, J = 0.4 Hz, 3H, methyl –CH_3), 2.7 (s, 1H), 3.0 (s, 1H), 5.6 (d, J = 12 Hz, 1H), 6.7 (t, J = 3.6 Hz, 1H), 7.4 (d, J = 4 Hz, 1H), 7.6 (d, J = 12 Hz, 1H). IR (ATR), ν_{max}/cm^{-1}: 3128, 3084 (w, aromatic C-H stretching), 2920, 2256 (w, aliphatic C-H stretching), 1610 (aromatic C=C stretching), 1481 (m, C=N stretching), 1263 (s, C-N stretching, 1068 (s, C-O stretching), 914 (s, =C-H twisting), 783 (s, aromatic C-H bending). Elemental analysis: anal. calcd. for $C_{10}H_{13}NOS$ (195.3): C 61.50 H 6.71 N 7.17; found: C 60.97 H 6.15 N 7.01.

Second step Appropriate compound synthesized from the first step of **Method B** (**i** or **ii**) (3.9 mmol) was taken into the reaction flask and it was dissolved in methanol (10 mL). After stirring the mixture for 10 min in an ice bath, the formation of dark brown solution was observed. $NH_2OH.HCl$ (0.295 g, 4.2 mmol) was poured into the solution and a color fading was observed. The ice bath was removed after a period of 10 min. The reaction was continued at room temperature and terminated after 24 h. The crude product was purified by column chromatography (solvent: ethyl acetate) to give the target compound.

5-(5-Methylfuran-2-yl)isoxazole (5): (yield: 75 %) dark brown oily solid ^{13}C-NMR (400 MHz, $CDCl_3$) δC/ppm: 13.6, 97.2, 108.1, 111.6, 141.6, 150.3, 154.5, 161.3. ^{1}H-NMR (400 MHz, $CDCl_3$) δH/ppm: 2.2 (s, 3H, methyl –CH_3), 6.2 (m, 1H), 6.4 (d, J = 2 Hz, 1H), 6.7 (d, J = 3.2 Hz, 1H), 8.2 (d, J = 2 Hz, 1H). MS (EI) m/z (%) calcd. for $C_8H_7NO_2$: 149.15; found: 150.14 (M + H) (LC): 5.68 min. (100 % ionization peak). IR (ATR), ν_{max}/cm^{-1}: 3158 (w, aromatic C-H stretching), 2951, 2846 (w, aliphatic C-H stretching), 1640 (s, aromatic C=C stretching), 1580,1508 (s, aromatic C=N stretching), 1286 (m, C-O stretching), 1196 (m, C-O stretching), 780 (s, C-H bending).

5-(5-Methylthiophene-2-yl)isoxazole (6): (yield: 57 %) brown oily solid ^{13}C-NMR (400 MHz, $CDCl_3$) δC/ppm: 15.3, 97.5, 126.3, 126.7, 127.1, 140.9, 150.6, 164.5. ^{1}H-NMR (400 MHz, $CDCl_3$) δH/ppm: 2.4 (s, 3H, methyl –CH_3), 6.2 (d, J = 1.6 Hz, 1H), 6.7 (t, J = 1.6 Hz, 1H), 7.2 (d,

J = 3.6 Hz, 1H), 8.1 (d, J = 1.6 Hz, 1H). MS (EI) m/z (%) calcd. for C_8H_7NOS: 165.21; found: 166.09 (M + H) (LC): 5.04 min. (100 % ionization peak). IR (ATR), ν_{max}/cm^{-1}: 3129, 3084 (w, aromatic C-H stretching), 2920, 2857 (w, aliphatic C-H stretching), 1611, 1593 (w, aromatic C=C stretching), 1481 (m, C=N stretching), 1249 (m, C-O stretching), 914 (m, N-O stretching), 780 (s, aromatic C-H bending).

Synthesis of isothiazole derivatives

In isothiazole synthesis, "thio-enamine" derivatives (**v** and **vi**) were synthesized instead of "keto-enamine" (**i** and **ii**) ones which were used as a starting material for the ring closure step in the formation of isoxazoles (Scheme 2). First step of the isothiazole synthesis was the synthesis of appropriate "keto-enamine" derivative as it was in the synthesis of the oxazoles. Second step was consisted of the transformation of "thio-enamine" derivatives, which were prepared at first step, into corresponding "perchlorate" salts with $POCl_3$ and $NaClO_4$. At the third step, "perchlorate" salt was transformed into appropriate "thio-enamine" derivative with $Na_2S.9H_2O$. At the fourth step, ring closure was completed with the reaction between hydroxylamine-o-sulfonic acid (HSA) and the "thio-enamine" derivatives which were obtained at the third step (Scheme 3). This procedure was entitled as **Method C**.

Method C

First step Previously synthesized appropriate prop-2-en-1-one derivatives (**i** or **ii**) (6.0 mmol) were dissolved in predistilled dichloromethane (15 mL) solution and added into a three-neck reaction flask. Then, $POCl_3$ (6.0 mmol) was added dropwise to the mixture with vigorously stirring. After 10 min, the ice bath was removed and the reaction flask was kept in the refrigerator for about 15 h. Following step included the removal of the solvent by rotary evaporator and the yellow colored oily residue was obtained. The content was washed with saturated solution of sodium perchlorate monohydrate (2.1 g) in water (5 mL) and the resulting solids (dark yellow-green colored) was vacuum filtered and washed with ethanol (10 mL).

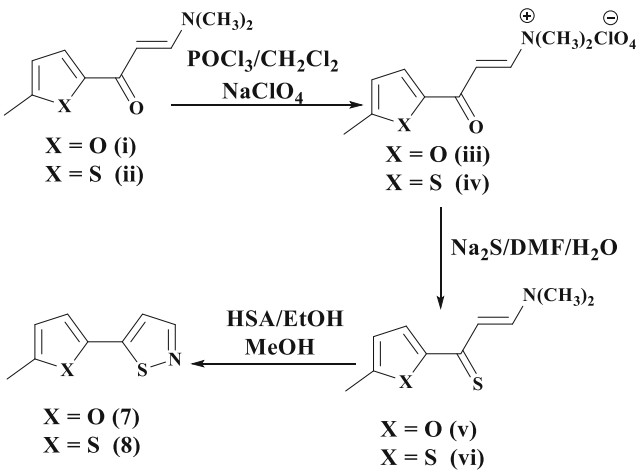

Scheme 3 Synthetic route to isothiazole derivatives (**7** and **8**).

(E)-3-(Dimethylamino)-1-(5-methylfuran-2-yl)prop-2-en-1-one, perchlorate salt (iii): (yield: 47 %, m.*p* > 250 °C) brown oily solid IR (ATR), ν_{max}/cm^{-1}: 3110 (w, aromatic C-H stretching), 2874 (w, aliphatic C-H stretching), 1644 (s, C=S stretching), 1590 (aromatic C=C stretching), 1550, 1426, 1292 (w, C-N stretching), 1188 (s, C-S stretching), 972 (m, =C-H twisting), 814 (s, aromatic C-H bending).

(E)-3-(Dimethylamino)-1-(5-methylthiophen-2-yl)prop-2-en-1-one, perchlorate salt (iv): (yield: 91.2 %, m.p > 250 °C) yellow solid IR (ATR), ν_{max}/cm^{-1}: 3078 (w, aromatic C-H stretching), 2856 (w, aliphatic C-H stretching), 1642 (m, C=S stretching), 1564 (m, aromatic C=C stretching), 1262 (s, C-N stretching, 1238, 1082 (s, C-O stretching), 812 (s, =C-H twisting).

Second step The corresponding perchlorate salt **(iii** or **iv)** (2.3 mmol) which was prepared in the preceding step was transferred to a round bottom one-neck flask and the system was placed into an ice bath. Pre-dried DMF (5 mL) was added dropwise into the yellow colored mixture. $Na_2S.9H_2O$ (2.3 mmol) solution was prepared by the addition of 1-mL pure water and poured into the reaction flask. Red-orange viscous solution was stirred for about 2 h at room temperature. After the dilution with 30 mL of water, the flask content was stored in the refrigerator overnight. The brick-red-colored precipitate was observed into the residual mixture and the crude product was then filtered off under vacuum.

(E)-3-(Dimethylamino)-1-(5-methylfuran-2-yl)prop-2-en-1-thione (v): (yield: 80 %, m.p: 142 °C) ^{13}C-NMR (400 MHz, $CDCl_3$) δC/ppm: 14.2, 38.2, 45.9, 106.6, 110.1, 118.1, 155.5, 157.4, 158.1. ^{1}H-NMR (400 MHz, $CDCl_3$) δH/ppm: 2.3 (s, 3H), 3.0 (s, 3H), 3.2 (s, 3H), 6.0 (d, J = 2.8 Hz, 1H), 6.6 (d, J = 12 Hz, 1H), 7.2 (s, 1H), 8.3 (d, J = 11.6 Hz, 1H). MS (EI) m/z (%) calcd. for $C_{10}H_{13}NOS$: 195.28; found: 196.10 (M + H) (LC): 4.50 min. (100 % ionization peak). IR (ATR), ν_{max}/cm^{-1}: 3100 (w, aromatic C-H stretching), 2910 (w, aliphatic C-H stretching) 1598, 1510, 1492 (aromatic C=C stretching), 1259 (m, C-O stretching), 947 (m, =C-H twisting), 788 (s, aromatic C-H bending). Elemental analysis: anal. calcd. for $C_{10}H_{13}NOS$ (195.3): C 61.50 H 6.71 N 7.17; found: C 60.86 H 6.47 N 7.08.

(E)-3-(Dimethylamino)-1-(5-methylthiophene-2-yl)prop-2-en-1-thione (vi): (yield: 74 %, m.p: 152 °C) ^{13}C-NMR

(400 MHz, $CDCl_3$) δC/ppm: 16.0, 38.1, 45.9, 107.0, 125.7, 126.6, 148.8, 152.2, 157.2. ^{1}H-NMR (400 MHz, $CDCl_3$) δH/ppm: 2.4 (s, 3H), 3.0 (s, 3H), 3.4 (s, 3H), 6.5 (d, J = 12 Hz, 1H), 6.7 (d, J = 2.8 Hz, 1H), 7.4 (s, J = 4 Hz, 1H), 8.3 (d, J = 11.6 Hz, 1H). MS (EI) m/z (%) calcd. for $C_{10}H_{13}NS_2$: 211.35; found: 212.05 (M + H) (LC): 4.67 min. (100 % ionization peak). IR (ATR), ν_{max}/cm^{-1}: 2922, 2850 (w, aliphatic C-H stretching), 1600, 1481, 1442 (aromatic C=C stretching), 1249 (m, C-O stretching), 814 (m, =C-H twisting), 771 (s, aromatic C-H bending). Elemental analysis: anal. calcd. for $C_{10}H_{13}NS_2$ (211.4): C 56.83 H 6.20 N 6.63; found: C 55.57 H 6.08 N 6.21.

Third step Corresponding starting materials (**v** or **vi**) (1.5 mmol) were dissolved in absolute ethanol (10 mL) and poured into a two-neck reaction flask fitted with a reflux condenser and it was placed into a hot water bath at 60 °C. Pyridine (3.0 mmol) was added dropwise by stirring to the red-colored solution over 10 min and the mixture was stirred for an extra 30 min at same temperature. Following the addition of HSA (1.5 mmol), the color of the mixture turned to tan within 2 h. After completion of the reaction, excess of ethanol was removed under pressure to give a yellow-brown oily solid.

5-(5-Methylfuran-2-yl)isothiazole (7): (yield: 57 %) yellow-brown oily solid ^{13}C-NMR (400 MHz, $CDCl_3$) δC/ppm: 13.6, 108.3, 109.9, 117.5, 144.5, 153.7, 156.0, 157.5. ^{1}H-NMR (400 MHz, $CDCl_3$) δH/ppm: 2.3 (s, 3H), 6.0 (d, J = 1.2 Hz, 1H), 6.5 (d, J = 3.2 Hz, 1H), 7.2 (d, J = 1.6 Hz, 1H), 8.3 (d, J = 1.2 Hz, 1H). MS (EI) m/z (%) calcd. for C_8H_7NOS: 165.21; found: 166.35 (M + H) (LC): 6.02 min. (100 % ionization peak). IR (ATR), ν_{max}/cm^{-1}: 3125 (w, aromatic C-H stretching), 2918 (w, aliphatic C-H stretching), 1605, 1555 (aromatic C=C stretching), 1478 (m, C=N stretching), 1240 (m, C-O stretching), 914 (m, =C-H twisting), 780 (s, aromatic C-H bending).

5-(5-Methylthiophen-2-yl)isothiazole (8): (yield: 62 %) yellow-brown colored oily solid ^{13}C-NMR (400 MHz, $CDCl_3$) δC/ppm: 15.3, 119.4, 126.4, 126.5, 130.2, 142.2, 157.8, 160.1. ^{1}H-NMR (400 MHz, $CDCl_3$) δH/ppm: 2.5 (d, J = 1.2 Hz, 3H), 6.7 (d, J = 1.2 Hz, 1H), 7.1 (d, J = 3.6 Hz, 1H), 7.2 (s, 1H), 8.3 (d, J = 2 Hz, 1H). MS (EI) m/z (%) calcd. for $C_8H_7NS_2$: 181.28; found: 182.10 (M + H) (LC): 5.84 min. (100 % ionization peak). IR (ATR), ν_{max}/cm^{-1}: 3078, 3140 (w, aromatic C-H stretching), 2914, 2855 (w, aliphatic C-H stretching), 1557 (w, aromatic C=C stretching), 1456 (m, C=N stretching), 812 (s, =C-H twisting), 795 (m, aromatic C-H bending).

Theoretical studies

As mentioned before, we aimed at comparing some experimental properties with theoretical values of the target compounds. For these purposes, chemical, electronic and spectral characteristics of our newly synthesized compounds were investigated with theoretical methods. All calculations were performed with Gaussian 09 W (Revision D.01) program package and GaussView 5.0.8 molecular visualization program [46, 47]. In the first step of the computational studies, the conformers which had the lowest energy values for each compound were determined by conformational analysis. The Density Functional Theory (DFT) [48] employed in scan calculations was B3LYP (Becke three-parameter hybrid correlation functional combined with Lee–Yang–Parr correlation functional) [49, 50] with 6-31G(d,p) basis set [51]. For the rest of the quantum chemical calculations, we applied similar methods which are used for this kind of molecules in the literature [52–54]. For the geometry optimization, target compounds in the ground state are computed by performing Hartree-Fock (HF) method [55] with the aug-cc-pVDZ basis set [56], DFT hybrid meta exchange-correlation functional (M06-2x) [57] at the aug-cc-pVDZ level and B3LYP method with the 6-31G(d,p), aug-cc-pVDZ, and cc-pVTZ [58] basis sets. All of these computational studies were performed in the gas-phase. Structural properties of the molecules (bond lengths, bond angles, dihedral angles, dipole moments, and polarizabilities), band gap energies and spectroscopic characteristics (UV-vis, FT-IR, ^{1}H-NMR and ^{13}C-NMR) were investigated and the results were assessed in detail. Following sections are organized based on these approaches and our outcomes set light to deeper understanding of the electrical and structural properties of the azole ring systems.

Structural analysis

A search for stationary points on the multidimensional PESs for azoles was performed with B3LYP/6-31G(d,p) level of theory. In order to obtain the different conformations, internal rotations around the C_5–C_6 single bond for the two-ring systems and the C_6–C_2 and C_5-C_{11} single bonds for the three-ring systems were performed, as can be seen in the geometry presented in Fig. 2, with the atoms numbered. For two-ring systems, two-dimensional (2D) PESs were obtained by changing the dihedral angle φ_1 from 0 and 360° with the increment of 60° without restriction of symmetry (Fig. 2). The dihedral angle φ_1 is defined by the atoms X_1-C_5-C_6-O_{10}. A rough geometry of the likely minimum energy structures could be guessed with the help of the PES and two local minimums (corresponding to syn- and anti-conformers) with respect to the C_5–C_6 single bond as shown in ESI† were obtained on the PES diagrams for the compounds **1**, **2**, **5**, **6**, **7**, **8**.

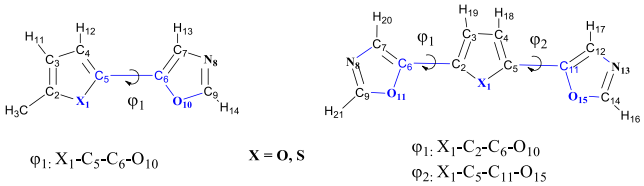

Fig. 2 Numbering atoms o1f target molecules for PES scan and definition of the dihedral angles. For clearance of the manuscript, illustration was presented here depicted only oxazole derivatives, but the same approach was used for preparing the scan analysis inputs of isoxazole and isothiazole derivatives

For the three ring systems, the three-dimensional (3D) potential energy surface of the molecules was obtained by varying the dihedral angles φ_1 and φ_2 (see Fig. 2). In this case, the dihedral angles φ_1 and φ_2 rotated from 0° to 360° with the increment of 60°. The dihedral angles φ_1 and φ_2 are defined by the atoms O_{11}-C_6-C_2-X_1 and X_1-C_5-C_{11}-O_{15}, respectively. Three possible structures (syn-syn, anti-anti, and syn-anti conformers) corresponding to a local minimum for the molecules **3** and **4** were obtained (see ESI†). These possible conformers were submitted to full geometry optimization using B3LYP/6-31G(d,p) level to find the most stable conformer. The conformers found with DFT were characterized as true minima on the potential energy surfaces by harmonic frequency analysis. The positive frequencies allowed us to determine the global minimum. The global minimum energy was found to be for the most stable conformer (anti) for each compound. The energy values for the anti-conformers 1, 2, 3, 4, 5, 6, 7, and 8 are −514.243, −837.218, −719.806, −1042.78, −514.209, −837.183, −837.213, and −1160.190 Eh, respectively. On the other hand, the energies of the syn conformers in which the ring heteroatoms oriented to the same direction are quite close to the energies of the anti-conformers and the energy values for syn conformers 1, 2, 3, 4, 5, 6, 7, and 8 are −514.241, −837.217, −719.801, −1042,78, −514.206, −837.183, −837.211, and −1160.180 Eh, respectively. It could be beneficial to underline that maximum energy difference between syn and anti-conformers are 0.010 Eh (6.28 kcal/mol). From the conformation analysis results, for each of our studied compounds, we selected only one conformation which had the lowest energy value and hence the most stable conformer (anti) and then, we continued with the lowest ones in subsequent calculations.

According to the conformational analysis and full geometry optimization results, for all of our cases, we observed that heteroatoms (oxygen or sulfur) that situated in oxazole, isothiazole, or isoxazole systems are in the opposite side to the other ring's heteroatoms—oxygen for the furan ring and sulfur for the thiophene ring—as expected. In other words, dihedral angle between those two heterocyclic rings is 180°. Similar results are observed for our three-ring systems containing oxazole derivatives (**3** and **4**). The ring's heteroatoms are oriented again towards different side and each dihedral angle between the two rings system is 180°. The calculated dihedral angles showed that all of the studied azole derivatives possessed a planar structure due to the stabilizing effects of the delocalization of non-bonding p electrons of oxygen, nitrogen, and sulfur atoms. That means the unpaired p electrons of the heteroatoms participate in the π-conjugation increased the stability of the ring systems. After determining the most stable conformers of the target compounds, the optimized geometries were recomputed with different calculation approaches in order to compare the accuracy of the calculations. Unless otherwise indicated, the results which were calculated with B3LYP/cc-pVTZ level of theory will be discussed in the following sections. The optimized structures for the global minimum are given in Fig. 3.

Bond length calculations Our literature search revealed that our target compounds are not present in any published computational or experimental studies. Therefore, we tried to compare our computational results with similar unsubstituted single-ring compounds (furan, thiophene, oxazole, isoxazole, or isothiazole). In order to make the comparison, we wanted to find the most appropriate method and basis set which calculate the bond lengths closest to the experimental bond lengths for unsubstituted five membered rings. Our results show that the B3LYP method with cc-pVTZ basis set is the most appropriate for calculation of the bond lengths for unsubstituted five-membered rings. Experimental and calculated bond lengths of some comparable heterocyclic compounds (Table 1) and our calculated bond lengths for the studied oxazole, isoxazole, and isothiazole derivatives are given in Tables 2 and 3, respectively. The calculated bond lengths of unsubstituted heterocyclic rings are in line with the experimental data.

As can be seen from Tables 2 and 3, the computed C-C bond lengths of the target compounds are in the range of 1.411–1.426 Å. The calculated C-C bond lengths for the corresponding unsubstituted five-membered heterocyclic rings are between 1.419 and 1.432 Å (Table 1). The C-C bond lengths between the ring's carbons that connect to the different rings are a little larger than that of ring's C-C bond lengths, which are between 1.430 and 1.444 Å. Due to the presence of conjugation between the two different ring systems, all these bonds have average C-C single and C=C double bond lengths, as expected. Moreover, the calculated C=C bond lengths of the molecules vary from 1.359 to 1.377 Å and similarly, calculated values of their primitive homologs are between 1.349 and 1.366 Å. The calculated C–C and C=C bond lengths of the studied compounds are in line with calculated values of thiophene, furan, oxazole, isoxazole, and isothiazole ring systems.

Generally, the C–N bond lengths are a bit shorter than the C–C bond lengths. The C-N and C=N bond lengths of the oxazole ring in two or three ring systems are calculated as about 1.384 and 1.287 Å, respectively. Furthermore, the

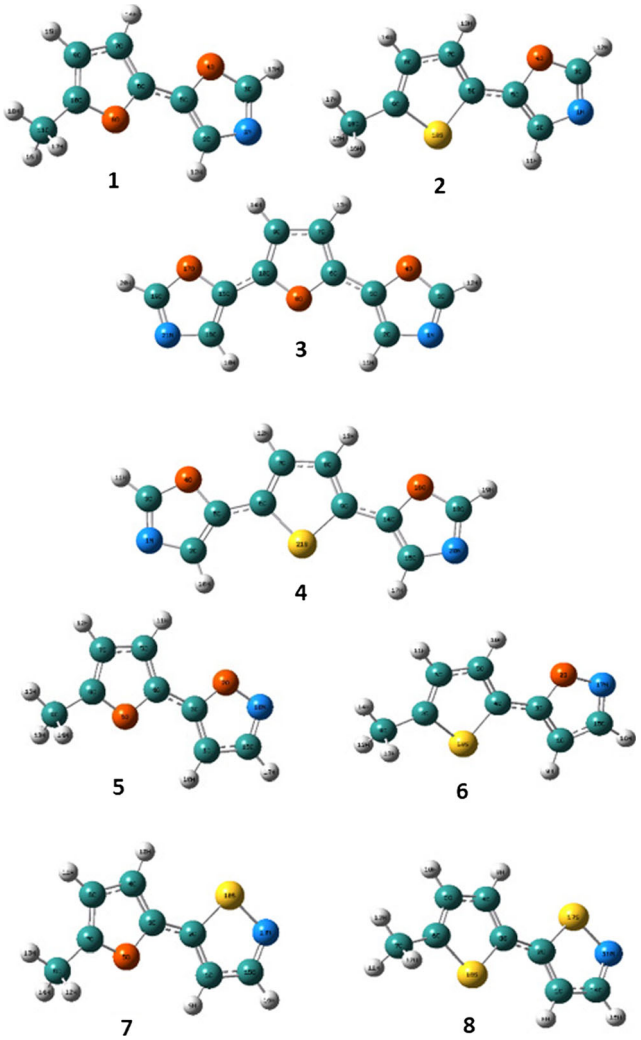

Fig. 3 The most stable conformers of target compounds

calculated values of the C-N and C=N bond lengths in unsubstituted oxazole ring are found 1.389 and 1.288 Å. The C=N bond lengths of unsubstituted isoxazole and isothiazole rings are calculated about 1.306 and 1.314 Å, respectively. These values are in line with the calculated values (1.305 and 1.314 Å) for unsubstituted isoxazole and isothiazole rings, respectively.

The C–O bond lengths are slightly shorter than the C–N bond lengths. The calculated C-O bond lengths are between 1.349 and 1.376 Å, and the calculated data for the corresponding unsubstituted derivatives are between 1.361 and 1.368 Å. The C-S bond lengths for thiophene and isothiazole in the studied molecules are between 1.738 and 1.749 Å and 1.735 and 1.738 Å, respectively, and their corresponding unsubstituted analogs' values are 1.726 and 1.713 Å. The computed N-O bond lengths of isoxazole derivatives are approximately 1.400 Å and the corresponding values for unsubstituted analogs are 1.397 Å. The calculated N-S bond lengths of isothiazole are approximately 1.666 Å and the calculations show that the bond lengths for the unsubstituted derivatives are about 1.664 Å. DFT calculation results [B3LYP/cc-pVTZ] are in good agreement with the experimental values for the unsubstituted heterocyclic rings (Table 1). Moreover, the calculated bond lengths of the studied azoles are also in line with the calculated values of the corresponding unsubstituted rings. However, there are very small differences between the bond lengths of the substituted and unsubstituted molecules. This is due to larger conjugation of two or three ring systems, which have different heteroatoms compared to a single ring system and also to their electronegativity characters.

Dipole moment and polarizability calculations Since our compounds' dipole moments and polarizabilities are not known yet, we wanted to see how these properties of this sort of ring systems change. It is also wanted to investigate the effects of calculation methods and the basis set on the electric properties. For these purposes, we studied the structure-dipole moment and polarization relationship for azoles. Dipole moment (μ) and polarizability (α) are, without doubt, among the most fundamental electrical properties. Therefore, calculation of these values with various theoretical models will provide a good basis for understanding the reliability of the calculation of the electronic states [65–67]. The electric dipole moments (μ) and the mean polarizabilities (ᾱ) of target compounds can be calculated by finite field method using different methods/basis sets. In order to calculate the electric dipole moments and the polarizabilities of the compounds, the origin of the Cartesian coordinate system (x, y, z) = (0, 0, 0) was chosen at the center of mass of the molecules. The total dipole moment μ, the mean polarizability ᾱ, and their x, y, z coordinates in components are defined below.

Dipole moment formula [68] is

$$\mu = \sqrt{\mu_x^2 + \mu_y^2 + \mu_z^2}$$

In the equation below, α is a second rank tensor property called the dipole polarizability and mean polarizability formula [69] is

$$\overline{\alpha} = \left(\alpha_{xx} + \alpha_{yy} + \alpha_{zz}\right) \Big/ 3$$

The calculated dipole moments and polarizabilities depend on a basis set and calculation method. Therefore, it is apparent that a large basis set and correlation is needed to get at reliable values. Since there is no information about the computational or experimental dipole moments and polarizabilities of the studied molecules in the literature, calculated dipole moments of the target compounds were again compared to their unsubstituted analogs. The calculated and experimental dipole moments of unsubstituted heterocyclic compounds (furan, thiophene, oxazole, isoxazole, or isothiazole) are given in Table 4 and their dipole

Table 1 Bond lengths determined by X-Ray and calculated by B3LYP/cc-pVTZ for the unsubstituted heterocyclic compounds (Å)

Bond type	Thiophene[a,b]	Furan[a,c]	Oxazole[d]	Isoxazole[e]	Isothiazole[f]	
C-C	1.423	1.431	–	1.425	1.397	*Exp.*
	1.424	1.432	–	1.420	1.419	*Calc.*
C=C	1.370	1.361	1.353	1.356	1.380	*Exp.*
	1.363	1.355	1.349	1.354	1.366	*Calc.*
C-N	–	–	1.395	–	–	*Exp.*
	–	–	1.389	–	–	*Calc.*
C=N	–	–	1.292	1.309	1.316	*Exp.*
	–	–	1.288	1.305	1.314	*Calc.*
C-O	–	1.362	1370	–	–	*Exp.*
	–	1.361	1.368	–	–	*Calc.*
C-S	1.714	–	–	–	1.715	*Exp.*
	1.726	–	–	–	1.713	*Calc.*
C-H	1.079	1.076	1.075	1.075	1.076	*Exp.*
	1.080	1.076	1.075	1.076	1.077	*Calc.*
N-S	–	–	–	–	1.661	*Exp.*
	–	–	–	–	1.664	*Calc.*
N-O	–	–	–	1.399	–	*Exp.*
	–	–	–	1.397	–	*Calc.*

[a] Reference [59]
[b] Reference [60]
[c] Reference [61]
[d] Reference [62]
[e] Reference [63]
[f] Reference [64]

moments are in the following order:

Isoxazole > isothiazole > oxazole > furan > thiophene

However, the calculated mean polarizabilities for unsubstituted derivatives are varied as thiophene, isothiazole, furan, isoxazole, and oxazole in descendent order. The results calculated by B3LYP/cc-pVTZ level of theory are in good agreement with available experimental dipole moments and polarizabilities for the unsubstituted derivatives.

The permanent dipole moments for the studied azoles are calculated with three different methods using three basis sets and the results are given in Table 5. The calculated data shows that dipole moment values of furan derivatives except oxazoles (1, 2) are higher than thiophene derivatives. By the guidance of Table 5, we could see that the calculated dipole moment values of the studied molecules are varied as isothiazole, isoxazole, and oxazole in descendent order, respectively. This result is in good agreement with previously given results for the unsubstituted derivatives. Calculations with different basis sets (6-31G(d,p), aug-cc-pVDZ, and cc-pVTZ) for the studied compounds give very similar results. Our result also shows that basis set effects are relatively lower but the electron correlation effects are dominant. For instance, the result obtained from DFT (B3LYP, MO6-2x) calculations gives different values in comparison to HF method. The dipole moments calculated with HF/aug-cc-pVDZ level of theory for oxazole derivatives are underestimated whereas for isoxazole derivatives are overestimated.

The mean polarizability ($\bar{\alpha}$) values of the studied compounds are calculated by using different methods and basis sets and the corresponding results are given in Table 6. The mean polarizability values of thiophene derivatives are higher than that of the furan derivatives and the polarities of the three-ring systems are higher than the two ring systems, as expected. According to obtained results, polarizability order for the studied azoles is similar to their corresponding unsubstituted derivatives and the order is

Table 2 Calculated bond lengths for oxazole derivatives (**1**–**4**) (Å)

Bond type	1		2		3		4	
	Furan moiety	Oxazole moiety	Thiophene moiety	Oxazole moiety	Furan moiety	Oxazole moiety	Thiophene moiety	Oxazole moiety
C-C	1.426	–	1.419	–	1.420	–	1.411	–
C-C[a]	1.432		1.437		1.430		1.435	
C=C	1.359	1.361	1.365	1.362	1.366	1.361	1.373	1.363
	1.363		1.370					
C-N	–	1.385	–	1.385	–	1.384	–	1.383
C=N	–	1.287	–	1.287	–	1.287	–	1.288
C-O	1.368	1.372	–	1.376	1.366	1.372	–	1.375
		1.358		1.356		1.357		1.356
C-S	–	–	1.741	–	–	–	1.743	–
			1.745					
C-H	1.075	1.076	1.079	1.076	1.075	1.075	1.079	1.076

[a] C-C bond lengths between the ring's carbons that connect to the different rings

Table 3 Calculated bond lengths for isoxazole and isothiazole derivatives (**5–8**) (Å)

Bond type	5		6		7		8	
	Furan moiety	Isoxazole moiety	Thiophene moiety	Isoxazole moiety	Furan moiety	Isothiazole moiety	Thiophene moiety	Isothiazole moiety
C-C	1.424	1.414	1.416	1.414	1.424	1.414	1.416	1.414
C-C[a]	1.434		1.440		1.436		1.444	
C=C	1.361 1.363	1.365	1.366 1.370	1.366	1.361 1.365	1.376	1.366 1.371	1.377
C=N	–	1.306	–	1.306	–	1.314	–	1.314
C-O	1.365 1.369	1.349	–	1.351	1.364 1.373	–	–	–
C-S	–	–	1.739 1.744	–	–	1.735	1.738 1.749	1.739
C-H	1.079	1.076	1.081	1.079	1.076	1.078	1.081	1.079
N-O	–	1.401	–	1.399	–	–	–	–
N-S	–	–	–	–	–	1.667	–	1.666

[a] C-C bond lengths between the ring's carbons that connect to the different rings

Isothiazole > isoxazole≈oxazole

However, the observed polarizability order for the studied compounds is different from their dipole moment order. The observed results could be explained by the interaction between atomic contributions, distance-dependent charge separation between heteroatoms, and number of resonance structures. The larger distance between charges should lead to a larger dipole moment of the compounds. Therefore, polarizability values of isothiazole compounds are higher than other compounds. On the other hand, the polarizability values obtained by different method and basis set are different. This means that basis set and electron correlation effects are important in calculation of the polarizabilities of the azoles. As can be seen from Table 6, HF/aug-cc-pVDZ level gives smaller values for the polarizabilities, while B3LYP/cc-pVTZ level gives higher values.

Table 4 Permanent dipole moment μ (Debye) and average polarizabilities ($\bar{\alpha}$) of unsubstituted heterocyclic compounds

Molecule	μ		$\bar{\alpha}$	
	DFT	Experiment	DFT	Experiment
Thiophene	0.52	0.533 ± 0.0005[a]	72.65	60.6[c], 65.2 ± 2.1[d], 66.1[e], 64.9 ± 0.6[f]
Furan	0.61	0.661 ± 0.006[b]	53.65	49.1 ± 2.2[d]
Oxazole	1.51	1.50[a]	48.44	
Isoxazole	2.94	2.90[a]	49.20	
Isothiazole	2.34	2.44 ± 0.2[a]	68.38	

[a] Reference [70]
[b] Reference [71]
[c] Reference [72]
[d] Reference [73]
[e] Reference [74]
[f] Reference [75]

Spectroscopic analysis

Computational and experimental UV-vis spectra The absorption spectrum is related to the molecular structure, and the relationship between the maximum absorption and the molecular structure is important in explaining the molecular properties. The time-dependent DFT (TD-DFT) is one of the most widely used methods in quantum chemistry because of its accuracy and relatively small computing time [76]. The method is able to detect accurate absorption wavelength and the calculated value corresponds to the vertical electronic transitions computed on the ground state geometry. Thus, we attempted to determine the maximum absorption peaks (λ_{max}) in the ultraviolet and visible (UV-vis) spectra of the studied compounds and then, we compared to our experimental and computational results.

Table 5 Dipole moments (μ, in Debye)

Entry	HF/aug-cc-pVDZ	M06-2x/aug-cc-pVDZ	B3LYP/6–31 G(d,p)	B3LYP/aug-cc-pVDZ	B3LYP/cc-pVTZ
1	2.541	2.675	2.679	2.815	2.680
2	2.584	2.520	2.485	2.667	2.787
3	1.016	2.962	2.891	2.982	2.887
4	1.056	2.448	2.395	2.408	2.354
5	4.054	3.805	3.844	3.986	3.855
6	4.343	3.654	3.612	3.815	3.678
7	4.022	3.747	3.930	3.973	3.778
8	4.154	3.655	3.789	3.870	3.677

Table 6 Calculated mean polarizability ($\bar{\alpha}$, in hartree)

Entry	HF/aug-cc-pVDZ	M06-2x/aug-cc-pVDZ	B3LYP/6–31 G(d,p)	B3LYP/aug-cc-pVDZ	B3LYP/cc-pVTZ
1	105.28	111.80	97.50	118.36	168.057
2	120.56	127.69	111.64	134.51	192.487
3	143.57	153.16	139.03	166.48	259.717
4	159.17	171.06	156.47	185.68	300.356
5	105.48	111.86	98.09	118.47	168.617
6	120.61	127.25	111.91	123.80	192.804
7	120.80	127.88	112.39	135.21	186.810
8	133.96	143.19	126.34	151.18	211.973

Calculations of λ_{max} for the target molecules in the gas phases are carried out with TD-DFT (B3LYP/6-31G(d,p)) method by using the same functions and basis sets, which were used in the geometry optimization. TD-HF method is also used in order to observe the variations between the computational methods. For the TD-DFT calculations, the Conductor-like Polarizable Continuum Model (CPCM) [77] is also used to take care of the solvent effects and CPCM-TD-B3LYP with 6-31G(d,p), 6-311++G(d,p), and cc-pVTZ basis sets in methanol solution is applied to the azole derivatives. On the basis of the fully optimized ground-state structure of the target compounds, vertical excitation energies, oscillator strength, and absorption wavelengths are obtained both in gas phase and methanol solution. The absorption spectra are simulated using GABEDIT program. The excited states are interpolated by a Lorentzian convolution with the full-width at half-maximum of 0.15 eV. The experimental and calculated λ_{max} values are given in Table 7 and their UV spectra are given in ESI†.

The observed and the calculated spectra of the azoles are between 290 and 319 nm and 291 and 361 nm, respectively, and azoles exhibit single absorption band in methanol. This result indicates that the excitations correspond to the electron transitions from the HOMO energy level to LUMO energy level and the excitations correspond to the π–π* transitions. Our results show that the λ_{max} values of the sulfur-containing derivatives (thiophene, isothiazole) shift to longer wavelengths relative to the corresponding values of the oxygen-containing derivatives (furan, oxazole, isoxazole). Moreover, the theoretical UV–Vis. spectra of the azoles in methanol are similar to those of gas phase with one band, but the lowest energy electronic transitions shift to a longer wavelength by approximately 10 nm because of the solvent effects.

In order to test the accuracy of the experimental and calculated absorption spectra for the azole derivatives, we compared our theoretical results with the experimental absorption spectra of the unsubstituted heterocyclic compounds. The experimental λ_{max} values for the unsubstituted furan, thiophene, oxazole, isoxazole, and isothiazole rings are 207, 237, 205, 215, and 245 nm, respectively, in methanol [78, 79]. It is well known that the substituents attached to the carbon atoms (C-2 or C-5 positions) of furan and thiophene rings affect the excitation energy. Because of the increasing effect on the π–electron density of the electron–donor substituents on C–2 or C-5 of furan or thiophene, the transition energies from HOMO to LUMO become lower and as a result of this, λ_{max} becomes longer. Therefore, it could be concluded that λ_{max} values of the two ring systems are significantly increased compared to the single ring derivatives. When the second ring system is attached to C–5 position of furan or thiophene ring (3 and 4), the molecules become larger, the conjugation increases, and the absorption bands shift to longer wavelengths. The calculated absorption bands of the molecules, except 3 and 4, are in line with their experimental values. λ_{max} values of the molecules (3 and 4) calculated by B3LYP with 6-31G(d,p), 6-311++G(d,p), and cc-pVTZ basis sets in methanol are greater than their experimental values. There are 16, 22; 29, 36; and

Table 7 Calculated vs. experimental UV absorption values (λ_{max}, nm)

	Gas Phase					Methanol			
Entry	TD-HF/aug-cc-pVDZ	TD-M062x/aug-cc-pVDZ	TD-B3LYP/6-31G(d,p)	TD-B3LYP/6-311++G**	TD-B3LYP/cc-pVTZ	TD-B3LYP/6-31G(d,p)	TD-B3LYP/6-311++G**	TD-B3LYP/cc-pVTZ	Experimental
1	266.11	269.7	276.99	279.84	280.86	293.43	291.19	291.12	290.00
2	281.53	285.55	291.6	295.38	297.35	302.31	303.58	305.10	301.00
3	305.39	309.73	325.62	324.73	329.52	324.34	337.02	341.33	308.00
4	326.31	331.18	345.76	344.25	350.27	341.81	354.99	360.99	319.00
5	265.93	270.24	276.15	278.9	280.2	296.16	295.6	292.69	292.00
6	279.06	284.02	290.29	292.13	294.38	295.56	303.9	303.09	298.00
7	284.63	292.78	299.66	302.39	303.59	312.77	320.31	317.73	308.00
8	295.45	302.78	309.54	303.35	313.21	319	317.87	323.88	310.00
R^2	0.90834	0.9437	0.8963	0.8723	0.8984	0.913	0.8935	0.9028	

Table 8 Calculated band gap energies (ΔEgap = ELUMO-EHOMO, in eV)

	Gas					Methanol
Entry	HF/aug-cc-pVDZ	M06-2x/aug-cc-pVDZ	B3LYP/aug-cc-pVDZ	B3LYP/cc-pVTZ	TD-B3LYP/cc-pVTZ	TD-B3LYP/cc-pVTZ
1	8.663	6.792	4.501	4.609	4.415 (39–40)	4.259 (39–40)
2	8.866	6.526	4.303	4.413	4.167 (43–44)	4.064 (43–44)
3	8.477	6.106	3.866	3.949	3.763 (52–53)	3.632 (52–53)
4	8.676	5.804	3.654	3.742	3.534 (56–57)	3.435 (56–57)
5	8.993	6.850	4.509	4.605	4.425 (39–40)	4.236 (39–40)
6	9.154	6.620	4.352	4.455	4.212 (43–44)	4.091 (43–44)
7	8.971	6.439	4.205	4.315	4.084 (43–44)	3.902 (43–44)
8	9.372	6.380	4.122	4.241	3.959 (47–48)	3.828 (47–48)

33, 42 nm differences between calculated and experimental absorption bands of the molecules (3 and 4), respectively. The 6-31G(d,p) basis set gives better results than the other two basis sets.

In order to consider the effect of calculation methods on absorption spectra, the calculated absorption wavelengths are plotted against the experimental values. As can be seen from the Table 7, the correlation coefficients (R^2) for the calculations with different methods in gas phase are between 0.87 and 0.94 and the corresponding value in methanol is almost 0.90. This close agreement between calculated and experimental values indicated that TD-B3LYP with 6-31G(d,p) basis set gives satisfactory result for understanding the absorption spectra of azoles.

In molecular interaction perspective, the Highest Occupied Molecular Orbital (E_{HOMO}) and the Lowest Unoccupied Molecular Orbital (E_{LUMO}) interacts with each other and they are accepted as the most significant energy levels [80, 81]. For our cases, the HOMO and LUMO energies and their energy difference ($\Delta E = E_{LUMO}\text{-}E_{HOMO}$) of the studied molecules are determined and the band gap energies are summarized in Table 8. It is well known that the energy of HOMO is related to the ionization potential whereas the energy of LUMO is related to the electron affinity. The energy gap reflects the chemical activity of molecules. In addition, the band gap is considered as a measure of the charge transfer and it is accepted as a relevant parameter in determining the molecular electrical transport property and the reactivity. If the energy gap between HOMO and LUMO decreases, then it will be easier to excite the electrons, which occupied the HOMO energy level. If the energy level of LUMO is low, it will be easier for LUMO to accept electrons, which excited from the HOMO energy level. As can be seen from the corresponding table, the computed results vary depending on the calculation method and basis set as expected.

The theoretical studies show that the band gaps are very similar for all optimized molecules and the values in gas phase are between 3.5 and 4.4 eV. However, the band gap values of isothiazole derivatives are found to be slightly lower than the other two systems. Additionally, for all derivatives, the band gap values vary from thiophene to furan ascending order. On the other hand, for the systems including two oxazole rings (**3**, **4**), in which the conjugated system becomes larger with the inclusion of second oxazole ring, the conjugation in the molecules increases and their band gaps decreases. The band gaps of two oxazole containing derivatives are dropped ~0.6 eV contrast to their two ring derivatives.

Computational and experimental FT-IR spectra In this part, the calculated harmonic vibrations of the target compounds are discussed and the results are compared with experimental FT-IR spectra. The harmonic vibrational wavenumbers and the absolute intensities are calculated by HF and DFT methods for the corresponding optimized geometries. There are 48 fundamental modes of vibrations associated with two-ring system and 57 for the three ring systems. Instead of discussing all individual modes, the most characteristic peaks are selected and the following explanations are made according to them. The scaled (scale factor: 0.965) [82, 83] fundamental vibrational wavenumbers of the target compounds are calculated with B3LYP/cc-pVTZ approach in gas phase and the results are given in Table 9. The frequencies calculated by DFT are smaller than the frequencies calculated by HF method due to electron correlation in density functional theory to a certain extent makes the frequency values smaller in comparison with the HF approach (see ESI†).

The presence of one or more heteroaromatic rings in a molecule are normally determined from the C-H and C=C ring vibrations. In this kind of organic compounds, the C-H IR stretching vibrations normally occur at 3100–3000 cm^{-1} [84]. The result calculated by B3LYP/cc-pVTZ shows that the vibrational wavenumbers in range of 3063–3167 cm^{-1} are assigned to aromatic C-H stretching

Table 9 Selected experimental and calculated (scaled) vibrational frequencies (cm^{-1}) and proposed assignments of the (a) oxazole derivatives (**1–4**) and (b) isoxazole and isothiazole derivatives (**5–8**)

Vibrational assignments	a								b							
	1		2		3		4		5		6		7		8	
	Exp.	Calculated	Exp.	Calculated	Exp.	Calculated	Exp.	Calculated	Exp.	Calculated	Exp.	Calculated	Exp.	Calculated	Exp.	Calculated
Aromatic C-H stretching	3140	3157, 3153 (o) 3149, 3133 (f)	3124, 30-76	3154, 3142 (o) 3106, 3082 (t)	3101, 2955, 2916, 2849	3158, 3155, 3144	3117	3154,3142 3113	3158	3167, 3150, 3134, 3116	3129, 3084	3156, 3116, 3108, 3083	3125	3141, 3129, 3116, 3063	3078, 30-40	3102, 3092, 3079, 3064
Aliphatic C-H stretching	2920	2921	2920, 28-57	2996, 2920	–	–	–	–	2951, 2849	3013, 2922	2920, 2857	2997, 2921	2918	3012, 2921	2914, 28-55	2996, 2921
C=C stretching	1635	1618, 1564	1611	1578, 1523	1516	1619, 1596	1659, 1611	1581,1559	1640	1615, 1558	1611, 1593	1578, 1520	1605, 1555	1588, 1536	1557	1544
C=N stretching	1585	1503	1535	1489	1456	1508, 1496	1518, 1491	1501,1484	1580, 1508	1497	1481	1471	1478	1470	1456	1470
C-O stretching	1204, 11-05 1082	1199 (f) 1097, 1087 (o)	1090	1093	1203, 1117, 1094, 1069, 1018	1102, 1098, 1091	1101, 1086, 1012, 988	1097,1096 1089,10-87	1286, 1196	1204, 1100, 966	1249, 1204, 1063, 1043	1241, 1053	1240, 1196, 1020	1200, 1047	–	–
C-S stretching	–	–	673, 63-7	650	–	–	665, 638	651	–	–	683	680	648	663	657	647
C-H bending	785	778	796	800	801	803	802	800	780	786	783	800	780	777	795	786
N-O stretching									916, 899, 868	914, 897, 864	914, 901	925, 902	–	–	–	–
N-S stretching									–	–	–	–	750	719	748	721

modes for the molecules **1–8**. The corresponding experimental values for the same molecules are between 2849 and 3158 cm^{-1}. The difference between the experimental and calculated vibrational wavenumbers could be attributed to the fact that the experimental results are taken in solvent phase while the theoretical results are obtained in gas phase. Another reason is harmonic approach used for calculations while, experimentally, many modes have highly anharmonic character.

The ring stretching vibrations of the heteroaromatic compounds are also extremely important. In several resources, highly characteristic peaks, which are observed for the aromatic compounds, are given in details [84]. In accordance with this information, carbon-carbon ring stretching vibrations occur in the region of 1430–1640 cm^{-1}. The experimental C=C stretching vibrations for the molecules **1–8** are observed in the range of 1516–1659 cm^{-1} and the calculated ring stretching vibrations (between 1520 and 1619 cm^{-1}) are in line with the experimental data.

It is well known that the C=N stretching vibration bands are generally observed in the range 1566–1672 cm^{-1}. The experimentally observed peaks between 1456 and 1585 cm^{-1} and the calculated bands between 1456 and 1508 cm^{-1} in FT-IR spectrum are identified as C=N vibrations of heterocyclic rings. Additionally, for the target compounds, the calculated C-N stretching modes are observed between 1359 and 1249 cm^{-1}. The corresponding experimental values are observed as a medium band at 1373 cm^{-1} and very strong band at 1250 cm^{-1} in FT-IR. Moreover, the C-O-C stretching vibrations generally occur in the range of 1050–1253 cm^{-1}. The experimental C-O stretching vibrations are measured in the range of 988–1286 cm^{-1} for molecules **1–8**, respectively. The corresponding calculated vibrations are between 966 and 1241 cm^{-1}.

The C-S symmetric and asymmetric vibrations of thiophene for molecules **2**, **4**, and **6** are calculated at 650, 651, and 680 cm^{-1}, respectively, and the C-S symmetric vibrations of isothiazole for compounds **7** and **8** are calculated at 663 and 647 cm^{-1}, respectively. The experimental C-S stretching vibrations of thiophene ring are observed at 673, 637; 665, 638, and 683 cm^{-1} and the C-S-N stretching vibrations for the isothiazole ring are also observed at 750 and 748 cm^{-1} for molecules **7** and **8**, respectively. The calculated frequencies at 719 and 721 cm^{-1} are assigned to C-S-N stretching vibrations for thiophene and isothiazole rings, respectively. N-O ring stretching vibrations are observed in the range of 868–916 cm^{-1} and the corresponding calculated values are between 864 and 914 cm^{-1}.

The aliphatic C-H stretching vibrations normally occur at 3100–2850 cm^{-1} and the C-H stretching vibrations of the methyl group connected aromatic rings are observed in the region of 2951–2849 cm^{-1}. Our calculated wavenumbers in the range of 3013–2920 cm^{-1} are assigned as C-H stretching of CH_3.

Computational and experimental ^{1}H-NMR and ^{13}C-NMR analysis In this section, we focused on the calculation of ^{1}H and ^{13}C chemical shifts of our studied molecules and by using their relevant experimentally determined shifts, we aimed to determine the best fitting computational method. As mentioned before, our experimental ^{1}H and ^{13}C magnetic resonance spectra are recorded in $CDCl_3$ solution and the calculated ^{1}H and ^{13}C NMR chemical shifts of the target compounds are obtained by the gauge-independent atomic orbital (GIAO) [85, 86] approach with B3LYP/6-31G(d,p) level of theory, which has precedent for NMR shielding tensor calculation especially in the case of reasonably larger molecules [85, 87]. It is well known that B3LYP method is strongly influenced by the basis set. Therefore, in order to assess the accuracy of the selected basis set, we also utilized a Dunning's correlation consistent basis set, cc-pVTZ with B3LYP which demands more computational efforts than 6-31G(d,p). For this purpose, first of all, the shielding of tetramethylsilane (TMS), which is used as a general standard, are calculated by using the selected calculation method and basis set. Then, the chemical shifting of the target molecules is calculated by using the same level of theory on fully optimized geometries. The extraction of the two evaluated values ($\sigma_{TMS} - \sigma_{calc.}$) gave the desired chemical shifts of the molecules. The calculated ^{1}H and ^{13}C isotropic chemical shielding of TMS at the B3LYP/6-31G(d,p) level in gas phase are 31.62 and 192.98 ppm, respectively. In the case of B3LYP/cc-pVTZ, the corresponding ^{1}H and ^{13}C isotropic chemical shielding values of TMS are calculated as 31.745 and 184.455 ppm. The experimental values for ^{1}H isotropic chemical shift and ^{13}C isotropic chemical shift for TMS are 30.84 and 188.1 ppm, respectively. The calculated values of ^{1}H and ^{13}C chemical shifts by B3LYP/6-3G(d,p) and B3LYP/cc-pVTZ methods in the gas phase together with experimental values are given in Table 10.

The aromatic protons of five-membered heterocyclic rings are normally observed in the range of 6–8 ppm; the methyl protons of these cyclic compounds give peaks between 2 and 2.5 ppm. Our measured and calculated corresponding protons are within the limits given above. The maximum deviation between the calculated and experimental values is 0.4 ppm, thus it is concluded that ^{1}H NMR chemical shifts calculated by using DFT method are in good agreement with the experimental values. The same trend is observed for the ^{13}C NMR, but the maximum deviation (±1.1) is higher than ^{1}H NMR chemical shifts. In order to evaluate the accuracy of the theoretical methods used in NMR calculations, we analyzed statistically the correlation between calculated and experimental chemical shifts. The correlations including both proton and carbon NMR results are given in ESI†. The correlations expressed by R^2 between measured and calculated NMR parameters are obtained ($y = ax + b$, a values close to 0.5 and R^2 values close to 1 for each studied compound. The correlation coefficients evaluated for each compounds are higher than 0.90 except for **4**.

Table 10 Experimental and calculated (a) ^{1}H-NMR chemical shifts (ppm) and (b) ^{13}C-NMR chemical shifts (ppm) of target molecules

a)

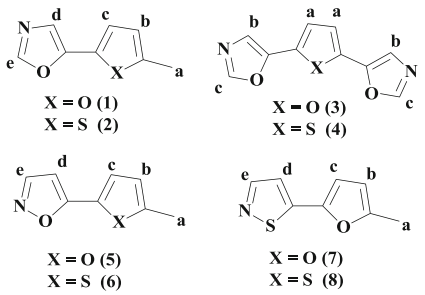

	1	2	3	4	5	6	7	8	
a	2.3	2.5	6.7	7.2	2.3	2.4	2.3	2.5	**Exp.**
	2.3	2.6	6.8	7.3	2.3	2.4	2.3	2.5	**Cal.**[a]
	2.4	2.6	6.9	7.4	2.4	2.6	2.4	2.6	**Cal.**[b]
b	6.1	6.5	7.3	7.3	6.2	6.2	6.0	6.7	**Exp.**
	6.2	6.4	7.5	7.5	6.3	6.2	6.2	6.7	**Cal.**[a]
	6.2	6.7	7.5	7.4	6.3	6.8	6.2	6.7	**Cal.**[b]
c	6.5	6.7	7.9	7.8	6.7	7.2	6.5	7.1	**Exp.**
	6.7	6.8	7.7	7.7	7.0	7.2	6.7	7.1	**Cal.**[a]
	6.7	7.2	7.7	7.7	7.1	7.6	6.8	7.2	**Cal.**[b]
d	7.1	7.0	–	–	6.4	6.7	7.2	7.2	**Exp.**
	7.4	6.9	–	–	6.4	6.7	7.2	7.2	**Cal.**[a]
	7.3	7.3	–	–	6.4	6.2	7.3	7.2	**Cal.**[b]
e	7.8	7.8	–	–	8.2	8.1	8.3	8.3	**Exp.**
	7.6	7.9	–	–	8.1	8.1	8.3	8.3	**Cal.**[a]
	7.6	7.6			8.2	8.1	8.3	8.3	**Cal.**[b]
	0.992	*0.998*	*0.907*	*0.871*	*0.995*	*1.000*	*0.998*	*1.00*	R^{2} [a]
	0.994	*0.923*	*0.923*	*0.871*	*0.994*	*0.926*	*0.998*	*1.00*	R^{2} [b]

b)

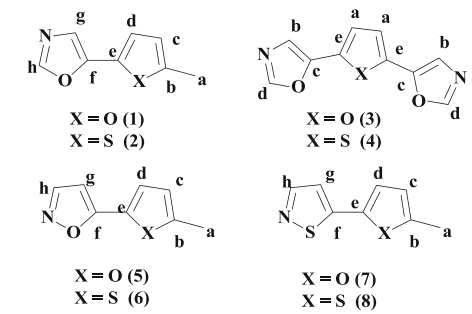

	1	2	3	4	5	6	7	8	
a	13.5	15.2	109.3	121.2	13.6	15.3	13.6	15.3	**Exp.**
	15.2	15.2	106.9	119.5	15.2	18.1	15.2	9.0	**Cal.**[a]
	15.1	17.7	113.3	128.4	15.2	17.9	15.1	17.8	**Cal.**[b]
b	149.5	147.1	122.3	125.1	150.3	140.9	153.7	142.2	**Exp.**
	141.7	150.9	120.2	120.1	144.4	144.6	148.3	136.4	**Cal.**[a]
	159.9	152.7	127.8	128.0	161.4	155.8	160.1	154.6	**Cal.**[b]
c	107.6	120.4	143.2	129.6	108.1	126.3	109.9	126.4	**Exp.**
	105.8	114.6	140.7	140.7	107.0	121.5	108.9	111.8	**Cal.**[a]
	113.1	130.3	151.3	154.4	113.7	131.1	113.8	130.9	**Cal.**[b]
d	108.6	124.6	150.2	150.1	111.6	126.7	117.5	126.5	**Exp.**
	106.5	120.6	142.6	143.7	109.4	121.6	111.7	112.1	**Cal.**[a]
	112.1	127.2	154.2	154.1	116.2	130.9	115.6	130.1	**Cal.**[b]
e	153.2	149.5	143.6	146.2	154.5	150.6	156.0	157.8	**Exp.**
	147.8	151.9	140.8	142.8	149.3	146.4	150.5	141.3	**Cal.**[a]
	151.5	141.9	152.0	141.2	151.6	141.2	154.1	145.9	**Cal.**[b]
f	141.6	127.1	–	–	161.3	164.5	157.5	160.1	**Exp.**
	139.9	133.4	–	–	157.0	159.9	157.6	153.2	**Cal.**[a]
	152.1	155.1	–	–	169.4	172.5	166.7	171.9	**Cal.**[b]
g	120.4	125.9	–	–	97.2	97.5	108.3	119.4	**Exp.**
	118.6	122.3	–	–	94.9	95.1	107.1	102.8	**Cal.**[a]
	125.9	126.4	–	–	99.2	99.8	119.4	130.2	**Cal.**[b]
h	144.2	140.9	–	–	141.6	127.1	144.5	130.2	**Exp.**
	141.3	144.8	–	–	140.0	133.4	142.6	128.7	**Cal.**[a]
	153.1	153.2	–	–	154.5	154.7	161.7	161.7	**Cal.**[b]
	0.999	*0.991*	*0.986*	*0.718*	*0.999*	*0.991*	*0.998*	*0.984*	R^{2} [a]
	0.993	*0.989*	*0.989*	*0.409*	*0.991*	*0.952*	*0.984*	*0.935*	R^{2} [b]

[a] B3LYP/6-31G(d,p) method

[b] B3LYP/cc-pVTZ method

Therefore, it can also be concluded that the GIAO method and B3LYP/6-31G(d,p) level of theory is sufficient to estimate ^{1}H and ^{13}C NMR chemical shifts values for our corresponding furan and thiophene derivatives.

Conclusions

Our present work represents joint experimental and theoretical studies of newly designed thiophene- or furan-based oxazole, isoxazole, and isothiazole derivatives. A convenient and efficient method is reported in order to synthesize azole derivatives with good to excellent yields. In a general point of view, it could be concluded that the obtained experimental results from this research are compatible with theoretical results. The results of the calculations done by DFT (B3LYP/cc-pVTZ) method for the bond lengths, bond angles, dipole moments, and polarizabilities are in line with their unsubstituted analogs. The calculated band gap values for all molecules are in a logical trend. Furthermore, spectral analyses of the target molecules are performed with consecutive experimental and theoretical calculations. Theoretical UV, IR, and NMR spectral analyses are done by different methods and basis sets. Due to the compatibility of the calculated and experimental results,

B3LYP method with 6-31G(d,p) basis set could be accepted as an appropriate method for the azole derivatives for understanding the corresponding spectral properties.

Acknowledgments Pervin Ünal Civcir would like to express her gratitude to AU-BAP (Project No: 13H4240002) for financial support. The numerical calculations reported in this research were performed at TUBITAK-ULAKBİM. High Performance and Grid Computing Center (TR-Grid e-Infrastructure).

References

1. Maertens JA (2004) History of the development of azole derivatives. Clin Microbiol Infect 10(Suppl 1):1–10. doi:10.1111/j.1470-9465.2004.00841.x
2. Linder J, Moody CJ (2007) The total synthesis of siphonazole, a structurally unusual bis-oxazole natural product. Chem Commun 1508–1509. doi: 10.1039/b618160k
3. Danilo D, Gloria S (2010) Thiazole and oxazole alkaloids: isolation and synthesis. Mar Drugs 8:2755–2780. doi:10.3390/md8112755
4. Yamada K, Yajima O, Yoshizawa Y, Oh K (2013) Synthesis and biological evaluation of novel azole derivatives as selective potent inhibitors of brassinosteroid biosynthesis. Bioorganic Med Chem 21:2451–2461. doi:10.1016/j.bmc.2013.03.006
5. Gomma GK (1998) Effect of azole compounds on corrosion of copper in acid medium. Mater Chem Phys 56:27–34. doi:10.1016/S0254-0584(98)00086-8
6. Mahdavian M, Ashhari S (2010) Mercapto functional azole compounds as organic corrosion inhibitors in a polyester-melamine coating. Prog Org Coatings 68:259–264. doi:10.1016/j.porgcoat.2010.04.002
7. Kovačević N, Kokalj A (2013) The relation between adsorption bonding and corrosion inhibition of azole molecules on copper. Corros Sci 73:7–17. doi:10.1016/j.corsci.2013.03.016
8. Hughes RA, Moody CJ (2007) From amino acids to heteroaromatics-thiopeptide antibiotics, nature's heterocyclic peptides. Angew Chem Int Ed 46:7930–7954. doi:10.1002/anie.200700728
9. Zhang J, Ciufolini MA (2011) An approach to the bis-oxazole macrocycle of diazonamides. Org Lett 13:390–393. doi:10.1021/ol102678j
10. Liu XH, Lv PC, Xue JY, Song BA, Zhu HL (2009) Novel 2,4,5-trisubstituted oxazole derivatives: synthesis and antiproliferative activity. Eur J Med Chem 44:3930–3935. doi:10.1016/j.ejmech.2009. 04.019
11. Zhou J, Jin J, Zhang Y, Yin Y, Chen X, Xu B (2013) Synthesis and antiproliferative evaluation of novel benzoimidazole-contained oxazole-bridged analogs of combretastatin A-4. Eur J Med Chem 68:222–232. doi:10.1016/j.ejmech.2013.08.006
12. Li YM, Milne JC, Madison LL, Kolter R, Walsh CT (1996) From peptide precursors to oxazole and thiazole-containing peptide antibiotics: microcin B17 synthase. Science 274:1188–1193. doi:10.1126/science.274.5290.1188
13. Dinarello CA (2010) Anti-inflammatory agents: present and future. Cell 140:935–950. doi:10.1016/j.cell.2010.02.043
14. Fernandes E, Costa D, Toste SA, Jose LF, Lima SR (2004) In vitro scavenging activity for reactive oxygen and nitrogen species by nonsteroidal anti-inflammatory indole, pyrrole, and oxazole derivative drugs. Free Radic Biol Med 37:1895–1905. doi:10.1016/j.freeradbiomed.2004.09.001
15. Boyd RE, Press JB, Rasmussen CR, Raffa RB, Codd EE, Connelly CD, Bennett DJ, Kirifides AL, Gardocki JF, Reynolds B, Hortenstein JT, Reitz AB (1999) Alpha(2) adrenoceptor agonists as potential analgesic agents. 1. (Imidazolylmethyl)oxazoles and -thiazoles. J Med Chem 42:5064–5071. doi:10.1021/jm990005a
16. Gürsoy A, Demirayak Ş, Çapan G, Erol K, Vural K (2000) Synthesis and preliminary evaluation of new 5-pyrazolinone derivatives as analgesic agents. Eur J Med Chem 35:359–364. doi:10.1016/S0223-5234(00)00117-3
17. Broom NJP, Cassels R, Cheng HY, Elder JS, Hannan PC, Masson N, O'Hanlon PJ, Pope A, Wilson JM (1996) The chemistry of pseudomonic acid. 17. Dual-action C-1 oxazole derivatives of pseudomonic acid having an extended spectrum of antibacterial activity. J Med Chem 39:3596–3600. doi:10.1021/jm950882q
18. Lu X, Liu X, Wan B, Franzblau SG, Chen L, Zhou C, You Q (2012) Synthesis and evaluation of anti-tubercular and antibacterial activities of new 4-(2,6-dichlorobenzyloxy)phenyl thiazole, oxazole and imidazole derivatives. Part 2. Eur J Med Chem 49:164–171. doi:10.1016/j.ejmech.2012.01.007
19. Stokes NR, Baker N, Bennett JM, Chauhan PK, Collins I, Davies DT, Gavade M, Kumar D, Lancett P, Macdonald R, Macleod L, Mahajan A, Mitchell JP, Nayal N, Nayal YN, Pitt GR, Singh M, Yadav A, Srivastava A, Czaplewski LG, Haydon DJ (2014) Design, synthesis and structure-activity relationships of substituted oxazole-benzamide antibacterial inhibitors of FtsZ. Bioorganic Med Chem Lett 24:353–359. doi:10.1016/j.bmcl.2013.11.002
20. Bull JA, Balskus EP, Horan RAJ, Langner M, Ley S V (2007) Total synthesis of potent antifungal marine bisoxazole natural products bengazoles a and b. Chem Eur J 13:5515–5538. doi:10.1002/chem.200700033
21. Ryu C-K, Lee RY, Kim NY, Song AL (2009) Synthesis and antifungal activity of benzo[d]oxazole-4,7-diones. Bioorg Med Chem Lett 19:5924–5926. doi:10.1016/j.bmcl.2009.08.062
22. Tomi IHR, Tomma JH, Al-Daraji AHR, Al-Dujaili AH (2015) Synthesis, characterization and comparative study the microbial activity of some heterocyclic compounds containing oxazole and benzothiazole moieties. J Saudi Chem Soc 19:392–398. doi:10.1016/j.jscs.2012.04.010
23. Moraski GC, Chang M, Villegas-Estrada A, Franzblau SG, Möllmann U, Miller MJ (2010) Structure–activity relationship of new anti-tuberculosis agents derived from oxazoline and oxazole benzyl esters. Eur J Med Chem 45:1703–1716. doi:10.1016/j.ejmech.2009.12.074
24. Sasahara K, Shimokawa Y, Hirao Y, Koyama N, Kitano K, Shibata M, Umehara K (2015) Pharmacokinetics and metabolism of delamanid, a novel anti-tuberculosis drug, in animals and humans: importance of albumin metabolism in vivo. Drug Metab Dispos 43:1267–1276. doi:10.1124/dmd.115.064527
25. Yale HL, Losee K (1966) 2-amino-5-substituted 1,3,4-oxadiazoles and 5-imino-2-substituted delta-2-1,3,4-oxadiazolines. A group of novel muscle relaxants J Med Chem 9:478–483. doi:10.1021/jm00322a007
26. Kempf DJ, Sham HL, Marsh KC, Flentge CA, Betebenner D, Green BE, McDonald E, Vasavanonda S, Saldivar A, Wideburg NE, Kati WM, Ruiz L, Zhao C, Fino L, Patterson J, Molla A, Plattner JJ, Norbeck DW (1998) Discovery of ritonavir, a potent inhibitor of HIV protease with high oral bioavailability and clinical efficacy. J Med Chem 41:602–617. doi:10.1021/jm970636+
27. Kang YK, Shin KJ, Yoo KH, Seo KJ, Hong CY, Lee CS, Park SY, Kim DJ, Park SW (2000) Synthesis and antibacterial activity of new carbapenems containing isoxazole moiety. Bioorg Med Chem Lett 10:95–99. doi:10.1016/S0960-894X(99)00646-0
28. Calí P, Nærum L, Mukhija S, Hjelmencrantz A (2004) Isoxazole-3-hydroxamic acid derivatives as peptide deformylase inhibitors and potential antibacterial agents. Bioorganic Med Chem Lett 14:5997–6000. doi:10.1016/j.bmcl.2004.09.087
29. Solankee A, Solankee S, Patel G (2008) Synthesis and antibacterial evaluation of some novel isoxazole and pyrazoline derivatives. Rasayan J Chem 1:581–585

30. Rahbaek L, Christophersen C (2001) The isoxazole alkaloids. Alkaloids Chem Biol 57:185–233. doi:10.1016/S0099-9598(01)57004-2
31. Conti P, Tamborini L, Pinto A, Sola L, Ettari R, Mercurio C, De Micheli C (2010) Design and synthesis of novel isoxazole-based HDAC inhibitors. Eur J Med Chem 45:4331–4338. doi:10.1016/j.ejmech.2010.06.035
32. Gehling VS, Hewitt MC, Vaswani RG, Leblanc Y, Côté A, Nasveschuk CG, Taylor AM, Harmange JC, Audia JE, Pardo E, Joshi S, Sandy P, Mertz JA, Sims 3rd RJ, Bergeron L, Bryant BM, Bellon S, Poy F, Jayaram H, Sankaranarayanan R, Yellapantula S, Bangalore SN, Birudukota S, Albrecht BK (2013) Discovery, design, and optimization of isoxazole azepine BET inhibitors. ACS Med Chem Lett 4:835–840. doi:10.1021/ml4001485
33. Künig G, Niedermeyer B, Deckert J, Gsell W, Ransmayr G, Riederer P (1998) Inhibition of [3H]α-amino-3-hydroxy-5-methyl-4-isoxazole-propionic acid [AMPA] binding by the anticonvulsant valproate in clinically relevant concentrations: an autoradiographic investigation in human hippocampus. Epilepsy Res 31:153–157. doi:10.1016/S0920-1211(98)00022-9
34. Bolvig T, Larsson OM, Pickering DS, Nelson N, Falch E, Krogsgaard-Larsen P, Schousboe A (1999) Action of bicyclic isoxazole GABA analogues on GABA transporters and its relation to anticonvulsant activity. Eur J Pharmacol 375:367–374. doi:10.1016/S0014-2999(99)00263-0
35. Stefan H, Feuerstein TJ (2007) Novel anticonvulsant drugs. Pharmacol Ther 113:165–183. doi:10.1016/j.pharmthera.2006.07.005
36. Epe C, Kaminsky R (2013) New advancement in anthelmintic drugs in veterinary medicine. Trends Parasitol 29:129–134. doi:10.1016/j.pt.2013.01.001
37. Carr JB, Durham HG, Hass DK (1977) Isoxazole anthelmintics. J Med Chem 20:934–939
38. White AD, Purchase CF, Picard JA, Anderson MK, Mueller SB, Bocan TM, Bousley RF, Hamelehle KL, Krause BR, Lee P, Stanfield RL, Reindel JF (1996) Heterocyclic amides: inhibitors of acyl-CoA:cholesterol O-acyl transferase with hypocholesterolemic activity in several species and antiatherosclerotic activity in the rabbit. J Med Chem 39:3908–3919. doi:10.1021/jm9604033
39. Burak K, Machoń Z (1992) Synthesis of isothiazole derivatives with potential biological activity. Pharmazie 47:492–495
40. Keck PE, Versiani M, Potkin S, West SA, Giller E, Ice K (2003) Ziprasidone in the treatment of acute bipolar mania: a three-week, placebo-controlled, double-blind, randomized trial. Am J Psychiatry 160:741–748. doi:10.1176/appi.ajp.160.4.741
41. Araki T, Yamasue H, Sumiyoshi T, Kuwabara H, Suga M, Iwanami A, Kato N, Kasai K (2006) Perospirone in the treatment of schizophrenia: effect on verbal memory organization. Prog Neuro-Psychopharmacology Biol Psychiatry 30:204–208. doi:10.1016/j.pnpbp.2005.10.015
42. Zificsak CA, Hlasta DJ (2004) Current methods for the synthesis of 2-substituted azoles. Tetrahedron 60:8991–9016. doi:10.1016/j.tet.2004.07.016
43. Roncali J, Garnier F, Garreau R, Lemaire M (1987) Reduction of the steric hindrance to conjugation in 3,4-disubstituted poly(thiophenes); cyclopenta[c]thiophene and thieno[c]thiophene as precursors of electrogenerated conducting polymers. J Chem Soc Chem Commun 19:1500–1502. doi:10.1039/c39870001500
44. Oldenziel OH, Leusen DV, Leusen AMV (1977) Chemistry of sulfonylmethyl isocyanides. 13. A general one-step synthesis of nitriles from ketones using tosylmethyl isocyanide. Introduction of a one-carbon unit. J Org Chem 42:3114–3118. doi:10.1021/jo00439a002
45. Leusen DV, Leusen AMV (2004) Synthetic uses of tosylmethyl isocyanide (TosMIC). Org React 57:417–666. doi:10.1002/0471264180.or057.03
46. Frisch MJ, Trucks GW, Schlegel HB, Scuseria GE, Robb M, Cheeseman JR, Scalmani G, Barone V, Mennucci B, Petersson GA, Nakatsuji H, Caricato M, Li X, Hratchian HP, Izmaylov AF, Bloino J, Zheng G, Sonnenberg JL, Hada M, Ehara M, Toyota K, Fukuda R, Hasegawa J, Ishida M, Nakajima T, Honda Y, Kitao O, Nakai H, Vreven T, Montgomery Jr JA, Peralta JE, Ogliaro F, Bearpark M, Heyd JJ, Brothers E, Kudin KN, Staroverov VN, Kobayashi R, Normand J, Raghavachari K, Rendell A, Burant JC, Iyengar SS, Tomasi J, Cossi M, Rega N, Millam JM, Klene M, Knox JE, Cross JB, Bakken V, Adamo C, Jaramillo J, Gomperts R, Stratmann RE, Yazyev O, Austin AJ, Cammi R, Pomelli C, Ochterski JW, Martin RL, Morokuma K, Zakrzewski VG, Voth GA, Salvador P, Dannenberg JJ, Dapprich S, Daniels AD, Farkas Ö, Foresman JB, Ortiz JV, Cioslowski J, Fox DJ (2009) Gaussian 09, Revision D.01. Gaussian, Inc., Wallingford CT
47. Dennington R, Keith T, Millam J (2009) GaussView, Version 5.0.8. GaussView, Version 5.0.8
48. Kohn W, Sham LJ (1965) Self-consistent equations including exchange and correlation effects. Phys Rev 140:A1133–A1A38
49. Becke AD (1988) Density-functional exchange-energy approximation with correct asymptotic-behavior. Phy Rev A 38:3098–3100. doi:10.1103/PhysRevA.38.3098
50. Lee C, Yang W, Parr RG (1988) Development of the Colle-Salvetti correlation-energy formula into a functional of the electron density. Phys Rev B 37:785–789. doi:10.1103/PhysRevB.37.785
51. Ditchfield R, Hehre WJ, Pople JA (1971) Self-consistent molecular-orbital methods. IX. An extended Gaussian-type basis for molecular-orbital studies of organic molecules. J Chem Phys 54:724–728. doi:10.1063/1.1674902
52. Ha TK (1979) A theoretical study of the electronic structure and properties of some five-membered heterocyclic compounds: pyrazole, imidazole, furan, isoxazole, 1,2,5-oxadiazole and 1,3,4-oxadiazole. J Mol Struct 51:87–98. doi:10.1016/0022-2860(79)80272-0
53. Pace A, Pierro P, Buscemi S, Vivona N, Barone G (2009) Experimental and DFT studies on competitive heterocyclic rearrangements. 3. A cascade isoxazole-1,2,4-oxadiazole-oxazole rearrangement. J Org Chem 74:351–358. doi:10.1021/jo802081k
54. Li LC, Wang XL, Cai WF, Tian AM (2011) Theoretical investigation on the reaction mechanism of aryl alcohols and p-toluenesulfonylmethyl isocyanide catalyzed by $InCl_3$. Comput Theor Chem 964:182–187. doi:10.1016/j.comptc.2010.12.020
55. Froese FC (1977) The Hartree-Fock method for atoms: a numerical approach. John Wiley and Sons, New York **ISBN 047125990X**
56. Dunning TH (1989) Gaussian basis sets for use in correlated molecular calculations. I. The atoms boron through neon and hydrogen. J Chem Phys 90:1007–1023. doi:10.1063/1.456153
57. Zhao Y, Truhlar DG (2008) The M06 suite of density functionals for main group thermochemistry, thermochemical kinetics, noncovalent interactions, excited states, and transition elements: two new functionals and systematic testing of four M06-class functionals and 12 other function. Theor Chem Accounts 120:215–241. doi:10.1007/s00214-007-0310-x
58. Kendall RA, Dunning TH, Harrison RJ (1992) Electron affinities of the first-row atoms revisited. Systematic basis sets and wave functions. J Chem Phys 96:6796–6806. doi:10.1103/PhysRev.136.B864
59. Schomaker V, Pauling L (1939) The electron diffraction investigation of the structure of benzene, pyridine, pyrazine, butatidene-1,3-cyclopentadiene, furan, pyrrole, and thiophene. J Am Chem Soc 61:1769–1780. doi:10.1021/ja01876a038
60. Hartough HD (2009) The chemistry of heterocyclic compounds, thiophene and its derivatives. John Wiley & Sons, New York

61. Bak B, Christensen D, Dixon WB, Hansen-Nygaard L, Andersen JR, Schottländer M (1962) The complete structure of furan. J Molec Spect 9:124–129
62. Kumar A, Sheridan J, Stiefvater OL (1978) The microwave spectrum of oxazole I. The complete structure by DRM microwave spectroscopy. Z Naturforsch 33a:145–152
63. Stiefvater OL (1975) The complete structure of isoxazole from naturally occurring isotopic forms by double resonance modulated microwave spectroscopy. J Chem Phys 64:2560. doi:10.1063/1.431647
64. Elgazwy ASH (2003) The chemistry of isothiazoles. Tetrahedron 59(38):7445–7463. doi:10.1016/S0040-4020(03)01070-6
65. Onsager L (1936) Electric moments of molecules in liquids. J Am Chem Soc 58:1486–1493. doi:10.1021/ja01299a050
66. Dzuba VA, Flambaum VV (2010) Current trends in searches for new physics using measurements of parity violation and electric dipole moments in atoms and molecules. arXiv:1009.4960
67. Gierke TD, Tigelaar HL, Flygare H (1972) Calculation of molecular electric dipole and quadrupole moments. J Am Chem Soc 94:330–338. doi:10.1021/ja00757a003
68. Berendsen HJC, Grigera JR, Straatsma TP (1987) The missing term in effective pair potentials. J Phys Chem 91:6269–6271. doi:10.1021/j100308a038
69. Guggenheim EA (1949) A proposed simplification in the procedure for computing electric dipole moments. Trans Faraday Soc 45:714. doi:10.1039/tf9494500714
70. McClellan AL (1974) Tables of experimental dipole moments. Rahara Enterprises, El Cerrito, CA
71. McClellan AL (1963) Tables of experimental dipole moments. Freeman WH, San Francisco, CA
72. Le Fe'vre CG, Le Fe'vre RJW, Rao BP, Smith MRJ (1959) Molecular polarisability. Ellipsoids of polarisability for certain fundamental heterocycles. J Chem Soc 1188–1192. doi: 10.1039/JR9590001188
73. Dennis GR, Gentle IR, Ritchie GLD, Andrieu CG (1983) Field-gradient-induced birefringence in dilute solutions of furan, thiophene and selenophene in cyclohexane. J Chem Soc Faraday Trans 2(79):539–545. doi:10.1039/F29837900539
74. Zhao MT, Singh BP, Prasad PN (1988) A systematic study of polarizability and microscopic third-order optical nonlinearity in thiophene oligomers. J Chem Phys 89:5535. doi:10.1063/1.455560
75. Coonan MH, Craven IE, Hesting MR, Ritchie GLD, Spackman MA (1992) Anisotropic molecular polarizabilities, dipole moments, and quadrupole moments of $(CH_2)_2X$, $(CH_3)_2X$, and C_4H_4X (X = 0, S, Se). Comparison of experimental results and ab initio calculations. J Phys Chem 96:7301
76. Stratmann RE, Scuseria GE, Frisch MJ (1998) An efficient implementation of time-dependent density-functional theory for the calculation of excitation energies of large molecules. J Chem Phys 109:8218. doi:10.1063/1.477483
77. York DM, Karplus M (1999) Smooth solvation potential based on the conductor-like screening model. J Phys Chem A 103:11060–11079
78. Van Veen EH (1976) Triplet $\pi \rightarrow \pi^*$ transitions in thiophene, furan and pyrrole by low-energy electron-impact spectroscopy. Chem Phys Lett 41:535–539. doi:10.1016/0009-2614(76)85411-5
79. Lang SA Jr, Lin Y (1984) In: Potts KT (ed) Comprehensive heterocyclic chemistry. Pergamon, New York
80. Scuseria GE (1999) Linear scaling density functional calculations with Gaussian orbitals. J Phys Chem A 103:4782–4790. doi:10.1021/jp990629s
81. Brus L (1986) Electronic wave functions in semiconductor clusters: experiment and theory. J Phys Chem 90:2555–2560. doi:10.1021/j100403a003
82. Sinha P, Boesch SE, Gu C, Wheeler RA, Wilson AK (2004) Harmonic vibrational frequencies: scaling factors for HF, B3LYP, and MP2 methods in combination with correlation consistent basis sets. Phys Chem A 108:9213–9217. doi:10.1021/jp073974n
83. Merrick JP, Moran D, Radom L (2007) An evaluation of harmonic vibrational frequency scale factors. J Phys Chem A 111:11683–11700. doi:10.1021/jp073974n
84. Silverstein RM, Bassler GC, Morrill TC (1991) Spectrometric identification of organic compounds. Wiley, New York
85. Wolinski K, Hinton JF, Pulay P (1990) Efficient implementation of the gauge-independent atomic orbital method for NMR chemical shift calculations. J Am Chem Soc 112:8251–8260. doi:10.1021/ja00179a005
86. Ditchfield R (1974) Self-consistent perturbation theory of diamagnetism. Mol Phys 27:789–807. doi:10.1080/00268977400100711
87. Cheeseman JR, Trucks GW, Keith TA, Frisch MJ (1996) A comparison of models for calculating nuclear magnetic resonance shielding tensors. J Chem Phys 104:5497. doi:10.1063/1.47178